Formation of Advanced Tokamak Plasmas without the Use of an Ohmic-Heating Solenoid

S. Shiraiwa,[1,*] S. Ide,[2] S. Itoh,[3] O. Mitarai,[4] O. Naito,[2] T. Ozeki,[2] Y. Sakamoto,[2] T. Suzuki,[2] Y. Takase,[1] S. Tanaka,[5] T. Taniguchi,[6] M. Aramasu,[1] T. Fujita,[2] T. Fukuda,[7] X. Gao,[8] M. Gryaznevich,[9] K. Hanada,[3] E. Jotaki,[3] Y. Kamada,[2] T. Maekawa,[10] Y. Miura,[2] K. Nakamura,[3] T. Nishi,[1] H. Tanaka,[10] K. Ushigusa,[2] and JT-60 Team

[1]*Graduate School of Frontier Sciences, University of Tokyo, Tokyo 113-0033, Japan*
[2]*Japan Atomic Energy Research Institute, Ibaraki 311-0193, Japan*
[3]*Research Institute for Applied Mechanics, Kyushu University, Fukuoka 816-8580, Japan*
[4]*School of Engineering, Kyushu Tokai University, Kumamoto 862-8652, Japan*
[5]*Department of Physics, Kyoto University, Kyoto 606-8502, Japan*
[6]*Graduate School of Science, University of Tokyo, Tokyo 113-0033, Japan*
[7]*Graduate School of Engineering, Osaka University, Osaka 567-0047, Japan*
[8]*Institute of Plasma Physics, Academia Sinica, Hefei, People's Republic of China*
[9]*EURATOM/UKAEA Fusion Association, Abingdon, OX14 3DB, United Kingdom*
[10]*Graduate School of Energy Science, Kyoto University, Kyoto 606-8502, Japan*

(Received 7 February 2003; published 21 January 2004)

A new operational scenario of advanced tokamak formation was demonstrated in the JT-60U tokamak. This was accomplished by electron cyclotron and lower hybrid waves, neutral beam injection, and the loop voltage supplied by the vertical field and shaping coils. The Ohmic heating (OH) solenoid was not used but a small inboard coil (part of the shaping coil), providing less than 20% of total poloidal flux, was used. The plasma thus obtained had both internal and edge transport barriers, with an energy confinement time of 1.6 times H-mode scaling, a poloidal beta of 3.6, and a normalized beta of 1.6, and a large bootstrap current fraction ($> 90\%$). This result opens up a possibility to reduce, and eventually eliminate, the OH solenoid from a tokamak reactor, which will greatly improve its economic competitiveness.

DOI: 10.1103/PhysRevLett.92.035001 PACS numbers: 52.50.Sw, 52.50.Gj, 52.55.Fa, 52.55.Tn

In conventional tokamak experiments, an Ohmic-heating (OH) solenoid located on the inboard side of the torus is used to start up the discharge and ramp up the plasma current (I_p) by induction. The need to equip an OH solenoid places severe restrictions on tokamak reactor design, e.g., by limiting the toroidal field strength and increasing the overall device size, resulting in a higher cost of electricity (COE). A reactor design study without an OH solenoid (OH less) [1] has shown that a fusion reactor with a COE comparable to present day power plants can be realized without operating in as high normalized beta (β_N) regime as assumed in conventional tokamak power plant designs [2,3] [β_N is defined as $\beta_t/(I_p a B_{t0})$, where $\beta_t \equiv 2\mu_0\langle p\rangle/B_{t0}^2$ is the toroidal beta, I_p is in MA, a[m] is the plasma minor radius, and B_{t0}[T] is the vacuum toroidal magnetic field at the plasma major radius $R = R_0$]. In particular, elimination of the OH solenoid is inevitable for a spherical tokamak (ST) reactor [4,5].

OH-less tokamak is a natural extension of the advanced tokamak (AT), which is a concept to improve the tokamak toward steady-state operation, consistent with the requirements of high β_N and high confinement. In AT, I_p needs to be maintained mostly by the self-generated bootstrap current I_{BS} [6], i.e., high bootstrap current fraction ($f_{\mathrm{BS}} \equiv I_{\mathrm{BS}}/I_p$), in order to reduce a certain level of poloidal beta β_p ($\equiv 2\mu_0 \int p\, dS/\int dS/B_p^2$, where the integrals are surface integrals over the poloidal cross section and B_p is the averaged poloidal field at the plasma boundary), while a low COE requires a certain level of β_t. Since β_N is limited by MHD stability, these two oppose each other and a self-consistent solution for conventional aspect ratio tokamak is known only when $q_{95} \leq 5$ ($q_{95} \simeq 10$ is acceptable in ST reactors [4]). In order to improve the credibility of an OH-less tokamak reactor design, an integrated OH-less scenario from plasma start-up to AT plasma with $q_{95} \leq 5$ must be demonstrated.

In OH-less tokamak operation, the vertical field (B_v) coils must provide both the poloidal flux and the vertical field. Hence, without other means, one cannot control the plasma shape and position and the plasma current independently (the latter is controlled by the OH solenoid in a conventional tokamak). Radio-frequency (rf) current drive techniques developed during the past two decades can be used as an independent knob to control the plasma current, separating the 2 degrees of freedom to some extent.

Plasma start-up and current ramp-up by a combination of electron cyclotron (EC) and lower hybrid (LH) waves was first demonstrated at the WT-2 tokamak (rf tokamak) [7] and extended by other experiments using either ECH, LH, or both waves [8–10]. Recently, a quasi-steady-state plasma was maintained for 30 s on the TRIAM-1M tokamak [11]. Noninductive current ramp-up efficiency was shown to be described well by the Fisch-Karney

 © 2004 The American Physical Society

theory [12,13]. As for approaching steady-state operation, the reversed shear (RS) plasma was theoretically predicted to be a promising configuration for high f_{BS} [14], and its production, sustainment, and control were achieved by LH current drive [15–17] and EC current drive [18,19]. Recently, it was shown that RS plasmas can have high f_{BS} under fully noninductively driven conditions [20,21]. In addition, it has been pointed out that B_v ramp-up during the increasing phase of β_p can provide an efficient means of ramping up the plasma current [22,23].

Thus far, these elements have been demonstrated separately. The rf tokamaks have been restricted to low densities and low plasma currents, while noninductive sustainment with high f_{BS} has been realized in OH-initiated higher density, higher current plasmas. This latter presents the first demonstration of integrating these ingredients into a single operational scenario. Although q_{95} was relatively high (12.8), the scenario presented here has produced a plasma with very high f_{BS} and high confinement (AT plasma) with less than 20% of total poloidal flux input from the coils located on the inboard side of the torus, i.e., a nearly OH-less condition.

The scenario consists of three phases, namely, the start-up phase, the low density noninductive current ramp-up phase by a combination of EC and LH waves, and the advanced tokamak phase with further I_p ramp-up by the combination of neutral beam injection (NBI) and B_v ramp-up. The experiment was carried out on the JT-60U tokamak [24] (Fig. 1). In these experiments, the poloidal flux generated by the VT and VR coils was used, while the OH solenoid current was kept constant at zero throughout the entire discharge. The VT coil set has a small inboard coil that must be eliminated in the future to demonstrate a complete OH-less operation. Because of the necessity of plasma shape control, this coil was used in the present experiment. The role of this inner coil and its small but finite flux contribution is discussed later. The flux provided by the divertor coil is small and negative (i.e., acts to reduce the plasma current).

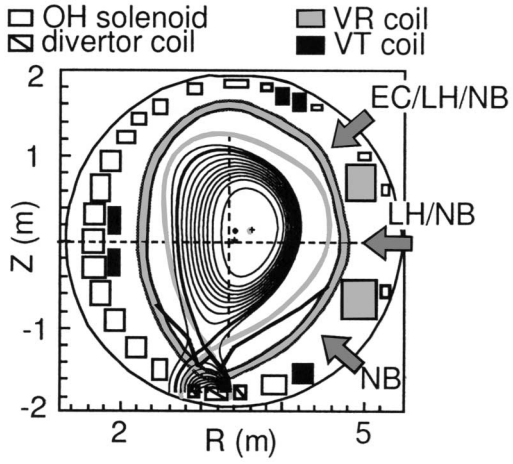

FIG. 1. Cross-sectional view of the JT-60U tokamak. VR (grey) and VT (black) coils are used to maintain equilibrium and control the plasma shape. The configuration shown in grey is used in the noninductive current ramp-up phase, while the black one is used in the advanced tokamak phase. The black one is a reconstructed equilibrium at $t = 8.5$ s of the discharge shown in Fig. 2.

An example of the integrated scenario is shown in Fig. 2 ($RB_t = 13.45$ Tm in this discharge). As 2 s, the currents in VT and VR coils were ramped linearly from -7.3 kA to $+6.5$ kA, and $+0.1$ kA to $+1.1$ kA, respectively, in 150 ms, where the negative current means the direction of current is opposite to that required to maintain the plasma in equilibrium. Such an operation was chosen to utilize the extra flux provided by the VT coil and to arrive at the correct B_V field to hold the plasma in equilibrium. The breakdown takes place at 2.1 s and the plasma current was ramped up to 0.2 MA using the ionization by EC (110 GHz) and LH (2 GHz) waves and induction by VT and VR coils.

It is noteworthy that the plasma current started up before the VT coil current returned to zero. The vacuum vessel eddy current induced by the VT and VR coils has a decay time constant of approximately 200 ms and further delays the inversion of the direction of B_v. Hence, toroidal equilibrium is not maintained during this period. In fact, the boundary reconstruction by a filament current model indicates that the plasma is limited by the outer wall and an attempt of equilibrium reconstruction was not successful before 2.5 s. In a discharge that had neither EC nor LH, I_p started rising only after the direction of B_v has

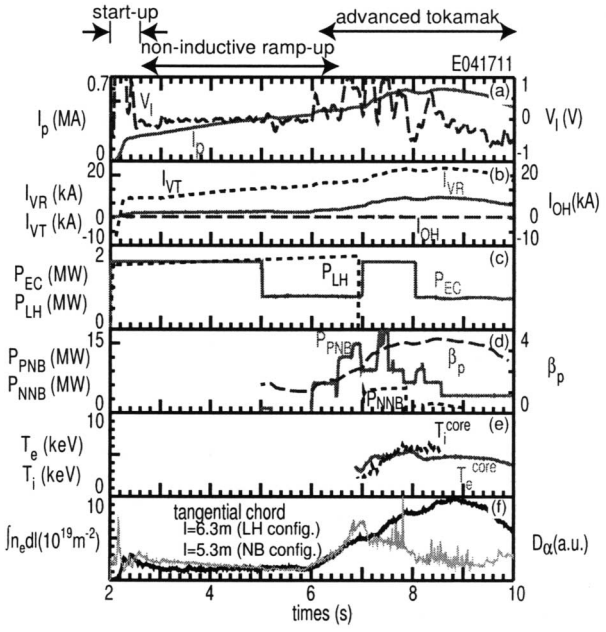

FIG. 2. An integrated OH-less scenario. (a) Plasma current (I_p) and loop voltage (V_1), (b) VT, VR, and OH coil currents, (c) LH/EC powers, (d) NBI powers and β_p, (e) core T_i and T_e, and (f) $\int n_e\, dl$ (black) and D_α (grey) emission.

turned positive, indicating that I_p start-up in the absence of a proper B_v for equilibrium is possible only in the presence of a strong source of plasma.

In the noninductive current ramp-up phase, I_p was ramped up to 0.4 MA by electron heating and current drive by LH and EC waves. A transition to a diverted configuration was accomplished by $t = 2.5$ s. Thereafter, the plasma configuration such as the X-point height and the plasma position were feedback controlled. The plasma configuration shown in grey in Fig. 1 was chosen for acceptable LH coupling, and the density was kept to a low level to provide a larger noninductively driven current. This intermediate phase is essentially the same as the well-documented case of noninductive current ramp-up. The conversion efficiency from the rf energy to the poloidal field energy $W_m = \frac{1}{2}(L_{\text{ext}} + L_{\text{int}})I_p^2$ for this case is $[(dW_m)/(dt) - P_{\text{ext}}]/(P_{\text{EC}} + P_{\text{LH}}) \simeq 2.2\%$, where the inductive contribution P_{ext} (about 40% of $(dW_m)/(dt)$ has been subtracted. Here, L_{ext} and L_{int} are the inductances calculated using the magnetic energy stored outside and inside plasma, respectively, and P_{ext} is total Poynting flux into the plasma due to external coils. The conversion efficiency is not optimized in this experiment and is lower than the previously reported values [9,13].

The transition from a low density plasma to a high density bootstrap dominated plasma was started when the plasma current became high enough to confine high energy ions produced by NBI. The plasma density was increased by gas puffing from 5.8 to 7 s to reduce the beam shine-through and 85 keV NBI was started at 6 s. Tangential NBI was switched on first because of its smaller shine-through fraction. Meanwhile, the equilibrium configuration is shifted inward from 6.5 to 7 s to allow more central NB power deposition and reduce the orbit loss. Perpendicular NBI started at 6.5 s under stored energy feedback control to avoid the β-limit disruption discussed later. Finally, the 377 keV negative ion based NBI started at 7.0 s. A combination of NB current drive and the flux input from VT and VR coils associated with B_p increase caused further plasma current ramp-up to 0.7 MA.

The plasma generated by this scenario had both an ITB and an edge transport barrier (H mode) [25]. In Fig. 3, the profiles of electron temperature (T_e) and electron density (n_e) measured by Thomson scattering, ion temperature (T_i) measured by charge-exchange recombination spectroscopy, and the safety factor (q) calculated from the equilibrium current density profile are shown. An evidence of ITB can be seen in the T_e profile during the current ramp-up phase ($t = 5.5$ s). The ITB is already formed at 3.0 s. ELM (edge localized mode) activities are observed in D_α emission after the transition to the advanced tokamak phase [Fig. 2(f)]. At the time of maximum stored energy ($t = 8.5$ s), a clear transport barrier can be seen in both ion and electron profiles with a large radius of ITB foot at a normalized radius $\rho = 0.7$. The q profile is deeply reversed with $q_{\min} = 5.6$ at $\rho = 0.7$ and

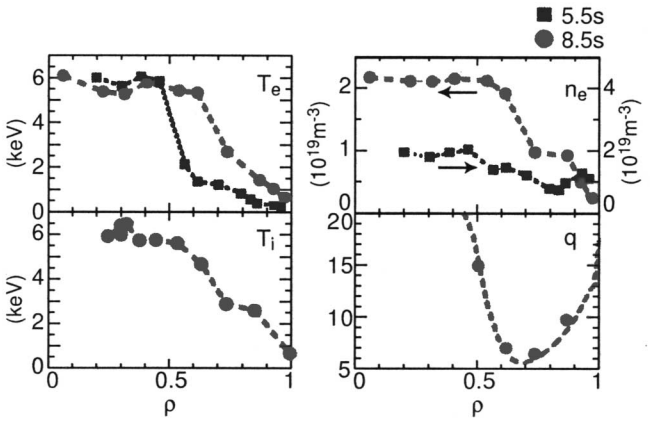

FIG. 3. Spatial profiles of T_e, T_i, n_e, and q in the LH/EC ramp-up phase (5.5 s) and the advanced tokamak phase (8.5 s).

$q_{95} = 12.8$. Plasma with $B_p = 3.6$ ($\epsilon B_p = 1$) and $\beta_N = 1.6$ is achieved at $\overline{n}_e = 0.5 n_{\text{GW}}$ ($\overline{n}_e$ is the line average density, and n_{GW} is the Greenwald density defined as $I_p[\text{MA}]/\pi a[\text{m}]^2$).

The central safety factor is high (at least 40) indicating the existence of a current hole [26,27]. The beam ion pressure gradient inside the current hole is not measured experimentally. In the present analysis, all gradients including the beam ion pressure gradient, and therefore the bootstrap current, are assumed to be zero inside the current hole ($p \leq 0.5$). In addition, a small but finite current density was assumed in the current hole region (indicated by the dashed total current density in Fig. 4). With these assumptions, the ACCOME current drive analysis code [28], using the NBI deposition and slowing down profiles calculated by the orbit following Monte Carlo (OFMC) code [29], and TOPICS 1.5-D transport code [30] yielded a bootstrap current fraction of $f_{\text{BS}} = 90\%$, which exceeds the highest value obtained thus far in JT-60U [21]. In Fig. 1, the reconstructed equilibrium at the time of maximum stored energy ($t = 8.5$ s) is overlaid. In the reconstruction, the current density term is modeled

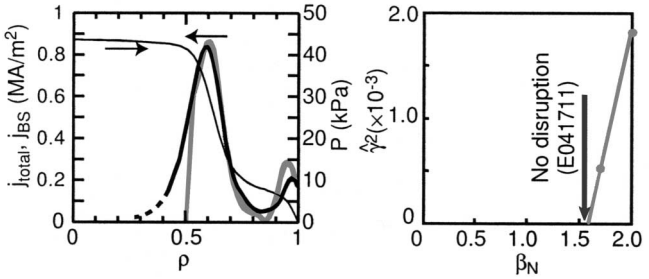

FIG. 4. Reconstructed pressure profile and current density profile (black) compared with the bootstrap current profile obtained by transport analysis (grey) at $t = 8.5$ s (left panel). Growth rate of the $n = 1$ kink-ballooning mode calculated by the ERATO code using the equilibrium profile at $t = 8.5$ s (right panel).

by a spline function and the motional Stark effect diagnostic is used as a constraint. The bootstrap current density calculated by this analysis is compared with the total current density calculated by equilibrium reconstruction in Fig. 4. The two profiles agree well with each other except in the H-mode pedestal region, indicating that the assumptions made in this analysis are acceptable. At the same time, an improvement factor over ITER98y2 ELMy H-mode energy confinement scaling ($H_{\mathrm{H98y2}} = 1.6$) evaluated by the summation of stored energy of the thermal electrons and thermal ions is 1.6, where the bulk ion density profile was obtained by subtracting the fast ion fraction evaluated by OFMC code from the total ion density profile obtained from the electron density profile and the measured Z_{eff} of 2.1.

Without feedback control of the NB injection power and at a slightly lower toroidal field strength ($RB_t = 12.78$ Tm), the plasma ended in a disruption. The β_N values for four such discharges were 1.7 just before disruption. A stability analysis by the ERATO code, assuming that both ∇p and $J_{\parallel}$ are nearly zero in the current hole region, predicted that the growth threshold for the $n = 1$ kink-ballooning mode is around $\beta_N = 1.6$, consistent with experimental observations (Fig. 4, right panel).

Although the inboard VT coil, which acts as a small OH solenoid, must be eliminated to reach the eventual goal of a complete OH-less tokamak reactor, the poloidal flux supplied by the inboard coil in this experiment was already small. Evaluation at $R = 3.4$ m, 0.46 Vs, 1.36 Vs, and 0.35 Vs was provided by the inboard VT coil, the outboard VT coil, and the VR coil, respectively, during the start-up phase. Hence, only 21% of the total flux was provided by the inboard coil. In contrast, in a normal start-up scenario using the OH solenoid, the inboard coils supply typically 70% of the total poloidal flux. Because this ratio is smaller during the later phases of the discharge, the poloidal flux contribution of the inboard coil to reach the maximum plasma current is significantly less than 20%. An important role played by the inboard coil in this experiment was to create a field minimum (''field null''). In a conventional aspect ratio tokamak, this function may be substituted by coils placed at the inboard top and bottom regions. As noted previously, plasma shape control by outer coils inevitable affects the plasma current in OH-less tokamak operation. The development of control techniques for such plasmas is not trivial, and needs to be developed.

Another remaining big challenge is to extend the present work (in which $q_{95} = 12.8$) to a lower q regime ($q_{95} \leq 5$). Extending the low density noninductive current drive phase is helpful but contradicts the purpose of reducing the COE. The plasma current ramp-up technique by β_V ramp-up reported in Refs. [22,23] may be used. Another possibility is bootstrap current overdrive ($f_{\mathrm{BS}} < 100\%$). The presented conservative estimate of f_{BS} does not exclude the possibility of 100% or even higher f_{BS}. Avoidance of the β limiting MHD instabilities may enhance the achievable β_p, resulting in more effective plasma current ramp-up by these techniques. The eigenfunctions of the destabilized mode are predominantly external in character, which may be stabilized by a close-fitting conducting wall.

In summary, an integrated advanced tokamak scenario without the use of the OH solenoid has been demonstrated on JT-60U. Plasmas having both ITB and ELMy H-mode transport barrier, with $\beta_p = 3.6$ ($\epsilon\beta_p = 1$), $\beta_N = 1.6$, and $H_{\mathrm{H98y2}} = 1.6$ has been obtained. A conservative estimate shows a very high bootstrap current fraction ($f_{\mathrm{BS}} = 90\%$). These results open up a possibility of improving the economic competitiveness of a tokamak reactor by eliminating the OH solenoid. In particular, it gives a great encouragement to the ST reactor for which OH-less operation is a necessity.

*Electronic address: shiraiwa@plasma.phys.s.u-tokyo.ac.jp
URL: http://plasma.phys.s.u-tokyo.ac.jp/index-e.html

[1] S. Nishio *et al.*, J. Plasma Fusion Res. **78**, 1218 (2002).
[2] F. Najmabadi *et al.*, Fusion Eng. Des. **38**, 3 (1997).
[3] K. Okano *et al.*, Nucl. Fusion **40**, 635 (2000).
[4] F. Najimabadi *et al.*, in *Fusion Energy 1998* (IAEA, Vienna, 1999), p. FTP/08.
[5] S. Nishio *et al.*, in *Proceedings of the 19th IAEA Fusion Energy Conference, Lyon, 2002* (IAEA, Vienna, 2002), pp. FT/P1–21.
[6] M. C. Zarnstorff *et al.*, Phys. Rev. Lett. **60**, 1306 (1988).
[7] S. Kubo *et al.*, Phys. Rev. Lett. **50**, 1994 (1983).
[8] K. Toi *et al.*, Phys. Rev. Lett. **52**, 2144 (1984).
[9] F. Jobes *et al.*, Phys. Rev. Lett. **52**, 1005 (1984).
[10] K. Ogura *et al.*, Nucl. Fusion **30**, 611 (1990).
[11] S. Itoh *et al.*, J. Plasma Fusion Res. **79**, 413 (2003).
[12] C. F. F. Karney *et al.*, Phys. Rev. A **32**, 2554 (1985).
[13] Y. Takase *et al.*, Phys. Fluids **30**, 1169 (1987).
[14] C. Kessel *et al.*, Phys. Rev. Lett. **72**, 1212 (1994).
[15] S. Ide *et al.*, in *Proceedings of the 16th IAEA Fusion Energy Conference, Montreal, 1996* (IAEA, Vienna, 1997), Vol. 3, pp. 253–264.
[16] X. Litaudon *et al.*, Plasma Phys. Controlled Fusion **38**, A251 (1996).
[17] C. D. Challis *et al.*, Plasma Phys. Controlled Fusion **43**, 861 (2001).
[18] P. Buratti *et al.*, Phys. Rev. Lett. **82**, 560 (1999).
[19] Z. A. Pietrzyk *et al.*, Phys. Rev. Lett. **86**, 1530 (2001).
[20] J. Hobirk *et al.*, Phys. Rev. Lett. **87**, 85002 (2001).
[21] T. Fujita *et al.*, Phys. Rev. Lett. **87**, 085001 (2001).
[22] O. Mitarai *et al.*, Nucl. Fusion **42**, 1257 (2002).
[23] O. Mitari *et al.*, Fusion Sci. Technol. **43**, 67 (2003).
[24] Special issue on *JT-60* [Fusion Sci. Technol. **42**, 179 (2002)].
[25] F. Wagner *et al.*, Phys. Rev. Lett. **49**, 1408 (1982).
[26] T. Fujita *et al.*, Phys. Rev. Lett. **87**, 245001 (2001).
[27] N. C. Hawkes *et al.*, Phys. Rev. Lett. **87**, 115001 (2001).
[28] K. Tani *et al.*, J. Comput. Phys. **98**, 332 (1992).
[29] K. Tani *et al.*, J. Phys. Soc. Jpn. **50**, 1726 (1981).
[30] H. Shirai *et al.*, J. Phys. Soc. Jpn. **64**, 4209 (1995).